applied sciences

MDPI

Article

Soil Mineral-Associated Organic Carbon and Its Relationship to Clay Minerals across Grassland Transects in China

Minshuang Zhao [1], Zhidan Zhang [1,*], Meijia Li [1], Chunyang Gao [1], Jinjing Zhang [1,*] and Nianpeng He [2,*]

[1] College of Resources and Environmental Science, Jilin Agricultural University, Changchun 130117, China; zms01574@163.com (M.Z.); limeijia19990123@163.com (M.L.); 18946737450@163.com (C.G.)
[2] Key Laboratory of Ecosystem Network Observation and Simulation, Institute of Geographic Sciences and Resources, Chinese Academy of Sciences, Beijing 100045, China
* Correspondence: zhidanzhang79@163.com (Z.Z.); zhangjinjing@126.com (J.Z.); henp@igsnrr.ac.cn (N.H.)

Abstract: The purpose of this study was to determine the mineral-associated organic carbon (MOC) and its relationship to clay minerals under different temperatures and precipitation. We selected three typical grassland transects in China: Titanium Plate (TP), Mongolian Plate (MP), and Loess Plate (LP) with natural temperature gradients. Along the transect, there is a gradient in the precipitation between the various types of grasslands. The surface soil (0–10 cm) was sampled to determine the MOC. Clay minerals were charactered by X-ray diffraction (XRD). According to the findings, the MOC content increased with decreasing temperature (5.41–14.89 g/kg). MOC had a positive correlation (r = 0.67) with the amount of clay mineral content. In the large-scale study of transects, precipitation masks the effect of temperature change on the MOC to a certain extent. It indirectly affected the MOC content by affecting the mixed-layer illite/smectite (I/Sme) content, and this effect was strongest at the lowest temperature TP (r = −0.73). Except for precipitation, CaO in the soil can affect soil organic carbon (SOC) stability by influencing the pH and I/Sme. The amount of bacteria increased as a result of I/Sme, and the influence of bacteria on the MOC was surpassed only by the soil pH. Climate and clay mineral composition characteristics affected the MOC to a certain extent. Among them, the effect of precipitation change on the MOC is higher than temperature, but it has little effect on soil with a higher weathering degree and CaO content.

Keywords: climate; mineral-associated organic carbon; clay mineralogy; spatial variation; grassland transects

Citation: Zhao, M.; Zhang, Z.; Li, M.; Gao, C.; Zhang, J.; He, N. Soil Mineral-Associated Organic Carbon and Its Relationship to Clay Minerals across Grassland Transects in China. *Appl. Sci.* **2024**, *14*, 2061. https://doi.org/10.3390/app14052061

Academic Editor: Fernando Rocha

Received: 16 February 2024
Revised: 24 February 2024
Accepted: 28 February 2024
Published: 1 March 2024

1. Introduction

Grasslands make up nearly 20% of the land surface area [1] and 12% of the Earth's organic matter [2]. Ecosystems of grasslands are crucial to the cycling and neutralization of carbon dioxide [3,4]. China's grassland area accounts for about 7% of the world's grassland area [5] and its carbon storage accounts for about 9–16% of the world's carbon storage [6]. Therefore, changes in soil organic carbon (SOC) stocks in Chinese grasslands are important for earth climate change and carbon cycle impact [7,8]. In general, SOC stability is directly related to endogenous soil properties (e.g., texture, clay minerals, organic matter, oxides) and is also influenced by exogenous factors (e.g., climate, land use, vegetation type, etc.) [9–11].

SOC is generally classified as reactive organic carbon and mineral-associated organic carbon (MOC) [12,13] linked to particles [14,15]. MOC is organic carbon complexed with soil mineral particles [16]. It is more stable [17] and has a longer turnover time. It accounts for a larger proportion of SOC [18]. Numerous factors, including the soil nutrient content, nutrient input, and land management practices, affect the concentration of MOC [19–22]. Among the main influencing factors are soil texture and mineral types [23,24]. Soil minerals have a large specific surface area and cation exchange capacity and soil texture is considered to be the dominant factor controlling MOC dynamics [17]. The soil microstructure and pore

system affect the stability of SOC [25]. In addition, clay minerals as soil skeletons [26] can influence the stability of SOC through surface interactions [27,28]. Different clay minerals have different abilities to adsorb and complex SOC [29]. Layered silicate minerals are effective in protecting SOC [30], with 2:1 minerals being more advantageous for SOC adsorption compared to 1:1 minerals [31]. The combination of clay minerals and oxides can promote the formation of aggregates [32] and improve the adsorption capacity of SOC [33]. A high soil pH can reduce the binding of minerals to SOC by affecting the electrical charge [30]. The effect of different grassland types on MOC varies, especially in the temperate zone and alpine grasslands, where there are differences in hydrothermal conditions and vegetation types [34,35]. The temperate zone and alpine grasslands provided the best environment to explore the influence of layered silicate mineralogy on MOC [36].

Gradient studies are an effective way to explore the influence of environmental conditions (i.e., climate, vegetation, soil) on the ecosystem [37]. While previous studies have focused on changes in a single grassland type or grassland SOC stocks, studies of temperature and precipitation gradients need to cover a large area. It is difficult to draw broad conclusions from small-scale field studies. Large-scale soil samples were gathered for this investigation along a gradient of temperature and precipitation. Natural gradients were used to explore the characteristics of MOC under different climates and its relationship with clay minerals. The influence of clay minerals on the stability of MOC under natural gradients was revealed. The relative contributions and interactions of different influences at large scales were considered. We hypothesized that soil clay minerals had an important impact on MOC content under large-scale studies. The correlation between soil clay minerals and MOC content was the result of multiple environmental variables. The purpose of the study was the following: (1) to determine the characteristics of the clay mineral composition and MOC of natural grassland transects in China; (2) to determine the correlation between clay minerals and MOC content in grassland soil on a large scale; (3) to quantitatively assess the important effects of environmental variables (climate, soil, bacteria) on clay minerals and MOC.

2. Materials and Methods

2.1. Studied Sites

Three typical transects in China were selected: the Tibetan Plateau (TP), Mongolian Plateau (MP), and Loess Plateau (LP) (Figure 1). The transects were selected as natural grasslands free from human activities (Table 1). The MP spans about 1000 km at 141–1249 m above sea level, with a mean annual temperature (MAT) of about 2.64 °C. The MP has a mean annual precipitation (MAP) from 168.29 to 448.47 mm. MP soil is mainly chestnut soil. The TP spans about 1600 km at 4037–4592 m above sea level. The MAT is about −2.91 °C and the MAP spans from 191.71 to 619.86 mm. TP soil is mainly brown soil. The LP spans about 800 km at an altitude of 792–1684 m above sea level. The MAT is about 8.70 °C and the MAP spans from 215.50 to 591.18 mm. LP soil is mainly cinnamon soil. Each transect covers meadow steppe (MS), typical steppe (TS), and desert steppe (DS) gradients with increased precipitation from west to east. The microorganism data (bacteria and fungi) are from Yang [38,39].

Ten representative sample areas were selected for each grassland transect. Eight sample quadrats (20 m × 20 m) were set up in each sample area. For every sampling quadrat, four randomly chosen plots (1 m × 1 m) were taken. A soil auger was used to gather soil samples ranging from 0 to 10 cm, which were then merged to create a composite sample. Soil samples were preserved after a 2 mm sieve.

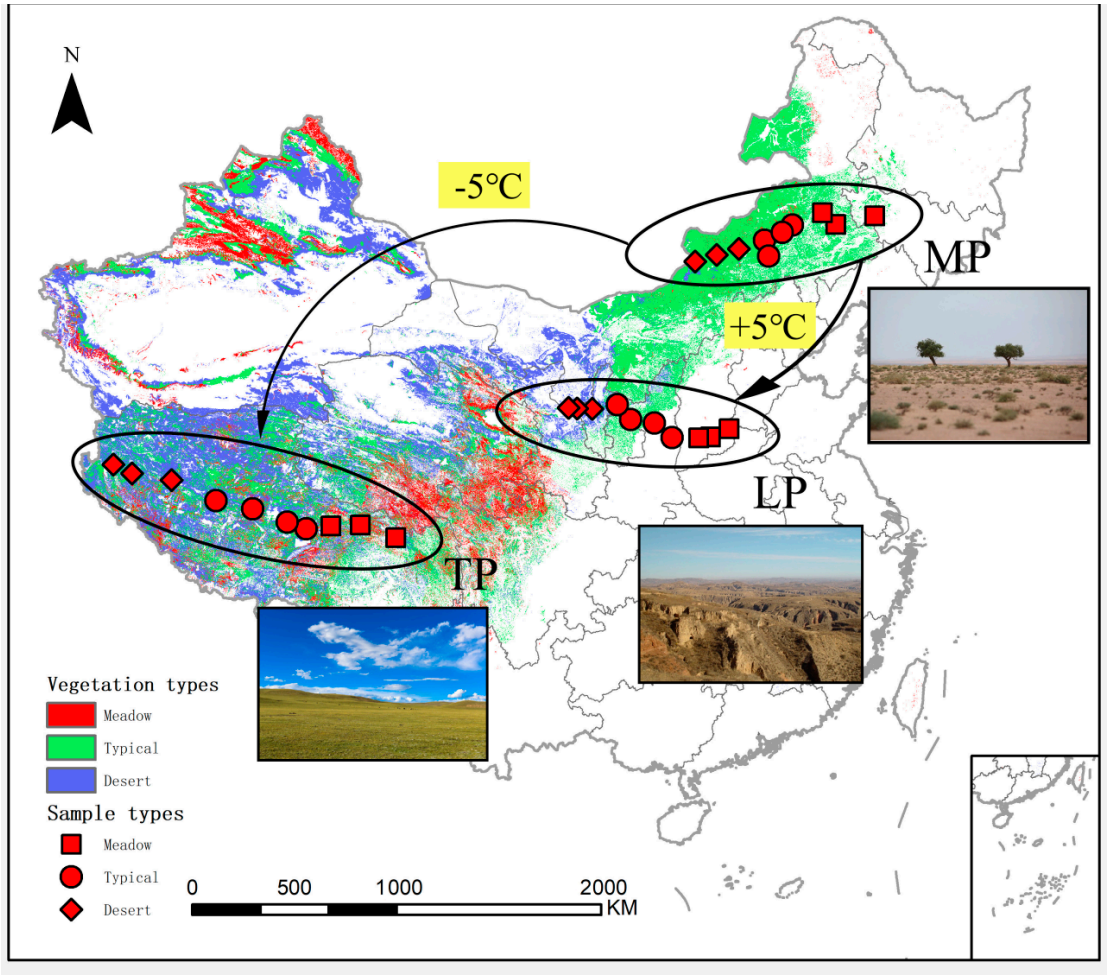

Figure 1. Location of grassland sampling sites in China. TP: Tibetan Plateau; MP: Mongolian Plateau; LP: Loess Plateau.

Table 1. Information on the study sites.

Transects	Grassland Type	Altitude (m)	MAP (mm)	MAT (°C)	pH
MP	MS	344	405.78	4.87	8.18
	TS	1108	362.39	0.96	7.59
	DS	1029	220.88	2.09	7.96
TP	MS	4292	552.67	−1.82	6.92
	TS	4640	433.99	−4.04	8.16
	DS	4415	266.75	−2.89	8.23
LP	MS	834	573.73	10.82	8.05
	TS	1291	466.37	8.23	8.09
	DS	1553	256.58	7.047	8.22

MAT: Mean annual temperature; MAP: Mean annual precipitation. TP: Tibetan Plateau; MP: Mongolian Plateau; LP: Loess Plateau. MS: Meadow steppe; TS: Typical steppe; DS: Desert steppe.

2.2. Soil Physicochemical Analyses

For the determination of the soil particle composition, 30% H_2O_2 was used to remove organic matter in ≤2 mm soil samples. Then the carbonate was removed with 10% HCl solution. The samples washed with deionized water were separated by the siphon method (according to Stokes' law). The separated samples were weighed after centrifugation and drying, and four particle grades were obtained: clay (<0.002 mm), sand (0.02–0.002 mm), and sand (2–0.02 mm). The combined percentages were used to classify soils using the

textural triangular coordinate map. The soil pH was measured with a pH meter by using a 1:5 (soil:water ratio) pH meter: Model PHS-3C (Yi Electrical Scientific Instrument Co., Ltd., Shanghai, China) [40]. The soil elements were determined using an X-ray fluorescence (XRF) spectrometer (XRF-1800, Shimadzu, Kyoto, Japan). The equipment was calibrated using the national standard GBW02103 [41,42]. The silica-alumina ratio (Sa) was expressed by $n(SiO_2)/n(Al_2O_3)$. The silica-sesquioxide ratio (Saf) is expressed by $SiO_2/(Al_2O_3 + Fe_2O_3)$.

2.3. SOC and MOC Analysis

An N/C Macro Elemental Analyzer 2100S (Analytik Jena AG, Jena, Germany) was used to measure the SOC content. The formula for calculating MOC concentration was MOC = SOC − Particulate organic carbon (POC) [43]. The POC content was determined with the Cambardella and Elliott method (1992) [44]. The 10 g sample was immersed in 30 mL 5 g/L of sodium hexaphosphate solution. Then it was dispersed on a reciprocating shaker at a low speed for 15 h (200 oscillations per minute). The sample was dispersed and passed through a 53 μm sieve and washed with distilled water until the water was completely clean. The soil particles retained on the sieve (representing particulate organic matter) were dried (60 °C) and weighed. Then, the soil was ground and sieved through a 150 μm sieve for the determination of organic carbon to determine the content of POC.

2.4. XRD Analyses

The dithionite-citrate-bicarbonate (DCB) method was used to remove iron from clay fraction (<2 μm). The iron-removed clay was saturated with 1 mol/L of CH_3COOK to make K-saturated air-dried film (K-air) and saturated with 1 mol/L $Mg(CH_3COO)_2$ to make Mg-saturated air-dried (Mg-air). The Mg-air was saturated with $C_3H_8O_3$ to make Mg-glycerol (Mg-gly). The K-air was heated in a muffle furnace at 300 °C and 550 °C for 2 h to make K-300 and K-550. The above samples were scanned using an XRD-7000 diffractometer (Shimadzu, Kyoto, Japan) under the following conditions: CuKa radiation (30.0 mA, 40.0 kV), scan range of 3–30°, and scan step of 0.02° [45]. Peak value extraction and semi-quantitative calculations were performed on the X-ray diffraction pattern using MID Jade 6.0. The relative content of minerals is evaluated based on the ratio between the characteristic reflection areas and the corresponding weight coefficient (Biscaye 1965; National Development and Reform Commission, 2006 [46]).

2.5. Statistical Analyses

We tested the significance of SOC, MOC, major element chemistry, and clay minerals under different grasslands transected by ANOVA using SPSS 22.0. A bubble diagram was created using the Origin 2019. Semi-quantitative calculations were carried out by MID Jade 6.0. The correlation coefficients between the MOC and clay minerals in several grassland transects, as well as the correlation between the MOC and environmental parameters (soil and climate), were clarified using Pearson's correlation (RStudio 4.0.3.). To investigate the impact of climate variables on MOC at a large scale, partial correlation analysis (SPSS 22.0) was used to control the influencing factors (MAP, pH, clay) to explore the relationship between the MOC and MAT. Regression models were used to screen and preliminarily determine the simple correlation relationships between influencing factors. Structural equation modeling (SEM) was further established after the regression analysis was used to eliminate the unimportant factors. SEM was used to test the causal relationship between the climate, soil properties, mineral species, and MOC. The degree of freedom (df), the p value, and the χ^2 test were used to assess the fit of this SEM model.

3. Results

3.1. Soil Physicochemical Properties

The classification of soil texture, based on various particle portions, is presented in Figure 2. The soil texture of the three grassland transects was between loamy and sandy, except for LP–MS (loamy) and MP–DS (sandy loam). The MP soil texture is loamy sandy

loam and sandy loam, the TP is loamy sandy loam, and the LP is sandy loam and loam. LP soil had the lowest soil texture dispersion compared to the other transects' soil. The texture of the different grassland types changes from sand to clay as the precipitation gradient increases. MP: MS–DS (sand = 71.92–84.20%), LP: MS–DS (sand = 32.98–61.61%), and TP: MS–DS (sand = 51.00–70.81%). MP: MS–DS (clay = 3.56–2.03%), LP: MS–DS (clay = 5.23–1.98%), and TP: MS–DS (clay = 3.08–4.54%). The texture of the three grassland transects changed from sandy to clay loam with increasing temperature. Clay: LP (7.92 ± 3.45%, CV% = 43.59) > MP (9.84 ± 5.38%, CV% = 54.70) > TP (10.68 ± 6.28%, CV% = 58.84). Sand: LP (63.67 ± 16.47%, CV% = 25.88) > MP (75.80 ± 12.15%, CV% = 16.03) > TP (50.48 ± 17.40%, CV% = 34.48).

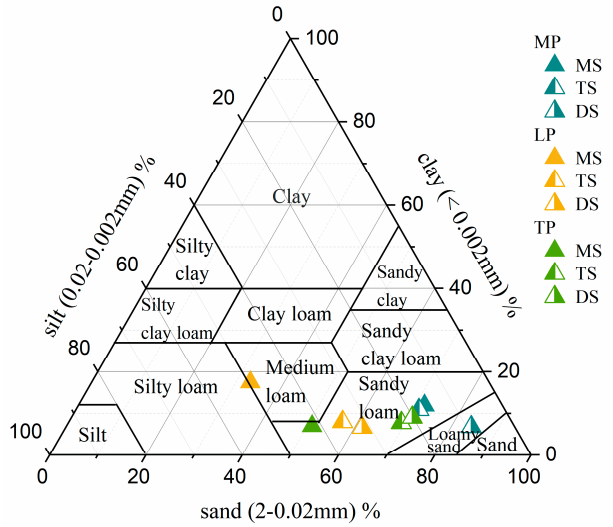

Figure 2. Soil textural classification of soil samples. TP: Tibetan Plateau; MP: Mongolian Plateau; LP: Loess Plateau; MS: Meadow steppe; TS: Typical steppe; DS: Desert steppe.

The soil chemical composition was dominated by SiO_2, Al_2O_3, and Fe_2O_3 in the MP and TP and by SiO_2, CaO, and Al_2O_3 in the LP (Table 2). The highest SiO_2 content (67.50 ± 4.10%) was found in the MP among the three transects. The lowest content of SiO_2 and Al_2O_3 in the three transects was LP soil (55.76 ± 3.01, 12.97 ± 1.42%). The highest content of CaO was LP soil (13.73 ± 3.19%). The coefficient of variation of LP soil chemical composition was the lowest among the three transects, except Al_2O_3 and Na_2O. Sa and Saf are important indicators to evaluate soil chemical weathering [47]. The MP had the highest Sa and Saf (8.33 ± 1.37, 6.77 ± 1.35), and the coefficient of variation of Sa and Saf was also the highest (16.44, 20.00). Therefore, the weathering degree of the MP is the lowest among the three transects.

Table 2. Major element chemistry of soil samples (%).

Transect		SiO_2	Al_2O_3	Fe_2O_3	TiO_2	MnO	CaO	MgO	K_2O	Na_2O	P_2O_5	Sa	Saf
MP	Mean	67.50 ± 4.10 a	14.00 ± 1.53 a	5.30 ± 1.58 b	0.96 ± 0.24 c	0.31 ± 0.17 a	3.28 ± 1.57 c	1.56 ± 0.35 b	4.76 ± 0.36 a	2.03 ± 0.35 a	0.20 ± 0.05 a	8.33 ± 1.37 a	6.77 ± 1.35 a
	CV%	6.08	10.91	29.80	24.82	55.29	47.88	22.36	7.64	17.33	26.94	16.44	20.00
TP	Mean	59.21 ± 5.19 b	14.36 ± 1.86 a	8.13 ± 2.58 a	0.97 ± 0.20 ab	0.16 ± 0.06 b	8.53 ± 7.31 b	2.34 ± 0.86 a	4.09 ± 0.82 b	1.50 ± 0.54 b	0.24 ± 0.09 a	7.10 ± 1.04 b	5.26 ± 0.93 b
	CV%	8.77	12.98	31.73	21.10	36.68	85.72	37.00	20.02	35.80	39.59	14.69	17.67
LP	Mean	55.76 ± 3.01 b	12.97 ± 1.42 a	8.32 ± 1.23 a	1.17 ± 0.12 a	0.16 ± 0.03 b	13.73 ± 3.19 a	2.60 ± 0.29 a	3.34 ± 0.18 c	1.55 ± 0.30 b	0.18 ± 0.03 a	7.39 ± 0.94 b	5.26 ± 0.77 b
	CV%	5.41	10.92	14.73	10.04	18.83	23.25	11.21	5.29	19.12	16.94	12.72	14.66

Lowercase letters indicate differences among the three transect soils at $p < 0.05$ level. TP: Tibetan Plateau; MP: Mongolian Plateau; LP: Loess Plateau. Sa: silica-alumina ratio; Saf: silica-sesquioxide ratio. CV%: Coefficient of variation among transects. Means ± standard errors.

3.2. SOC and MOC in Different Grassland Transect Soils

The average content of SOC from the three grassland transects was TP 21.08 g/kg, MP 12.39 g/kg, and LP 8.12 g/kg. The average content of MOC was TP (14.89 g/kg) > MP (8.07 g/kg) > LP (5.41 g/kg) (Figure 3a). The average value of MOC/SOC in LP soil was the highest (66.67%), and the average value of MOC/SOC in MP was the lowest (65.33%), while the TP was 65.99% (Figure 3b). Generally, the MOC content of the tested soil decreased with the increase in the temperature gradient. The highest MOC content in the three transects was the TP transect MS (36.63 g/kg), and the lowest was the TP transect DS (2.60 g/kg). The grassland type with the lowest MOC content in each transect was the DS.

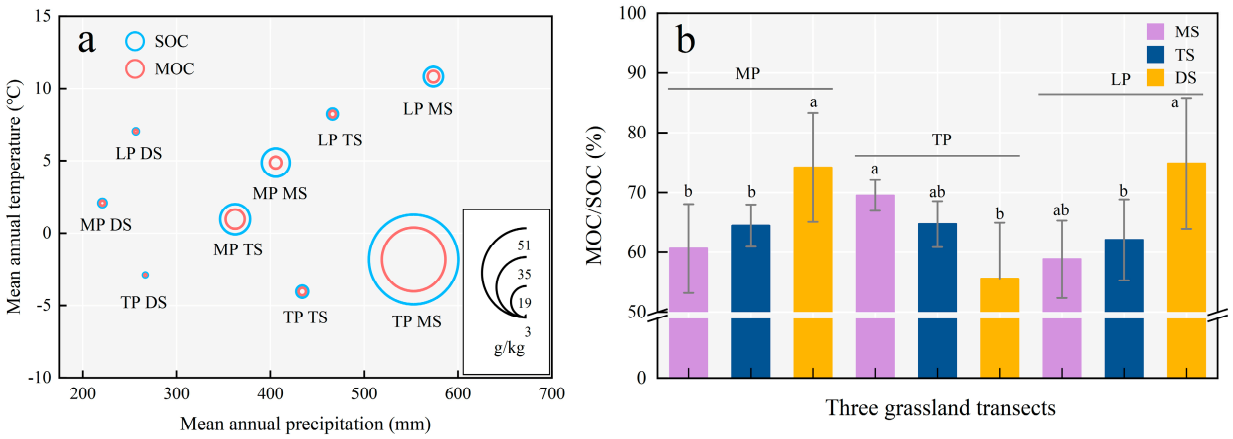

Figure 3. SOC and MOC content of grassland transects soil (**a**) SOC and MOC, (**b**) MOC/SOC. Lowercase letters indicate differences among the three grassland type MOC/SOC value at $p < 0.05$ level. TP: Tibetan Plateau; MP: Mongolian Plateau; LP: Loess Plateau; MS: Meadow steppe; TS: Typical steppe; DS: Desert steppe; SOC: soil organic carbon; MOC: mineral-associated organic carbon.

3.3. Clay Minerals Component Characteristics

The main minerals in the three grassland transects were smectite (Sme) (29.31–40.37%), illite (It) (37.27–60.82%), vermiculite (Ver) (0.72–9.34%), mixed-layer illite/smectite (I/Sme) (2.06–33.27%), kaolinite (Kao), and chlorite (Chl) (Figure 4). Kao and Chl contents were less than 1%. The highest contents of Sme and It in the LP were 34.54 ± 3.71% and 53.00 ± 9.16%, respectively. The highest contents of Ver and I/Sme in the MP were 4.96 ± 7.94% and 21.75 ± 9.84%, respectively.

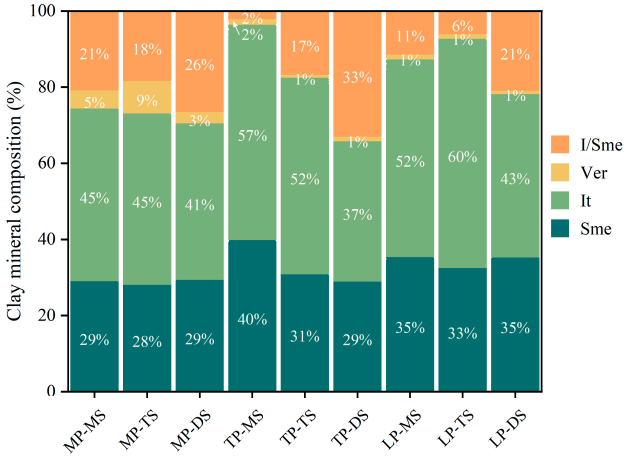

Figure 4. Spatial variation in mineralogy in the clay fraction. Sme: smectite; It: illite; Ver: vermiculite; I/Sme: mixed-layer illite/smectite.

3.4. Linking MOC to Clay Minerals and Other Factors

The MOC content was positively correlated with the environmental factor MAP (r = 0.53), clay (r = 0.67), silt (r = 0.47), bacteria (r = 0.67), and fungi (r = 0.56). MOC content with pH (r = −0.58), Sa (r = −0.40), Saf (r = −0.42), and sand (r = −0.58) was negatively correlated (Table 3). The correlation between the above indicators and MOC was stronger than SOC (except bacteria and fungi).

Table 3. Pearson's correlation among soil physical-chemical, environmental factors, and MOC.

	SOC	MOC	pH	Clay	Silt	Sand	MAP	MAT	SiO_2	Al_2O_3	Fe_2O_3	CaO	Sa	Saf	Bacteria	Fungi
SOC		0.99	−0.70	0.64	0.43	−0.55	0.57	−0.08	0.01	0.43	0.38	−0.28	−0.33	−0.37	0.70	0.60
MOC			−0.69	0.67	0.47	−0.58	0.53	−0.07	−0.03	0.48	0.43	−0.27	−0.40	−0.42	0.67	0.56
pH				−0.22	0.06	0.04	−0.21	0.20	−0.50	−0.36	−0.07	0.74	−0.02	−0.01	−0.54	−0.51
Clay					0.63	−0.78	0.37	0.18	−0.33	0.54	0.55	0.06	−0.61	−0.60	0.33	0.32
Silt						−0.95	0.59	0.36	−0.72	0.17	0.86	0.40	−0.59	−0.79	0.16	0.10
Sand							−0.57	−0.37	0.64	−0.26	−0.82	−0.32	0.61	0.76	−0.20	−0.15
MAP								0.18	−0.29	0.03	0.46	0.17	−0.19	−0.38	0.40	0.34
MAT									−0.30	−0.31	0.19	0.29	0.02	−0.09	−0.65	−0.69
SiO_2										0.08	−0.65	−0.84	0.62	0.70	0.08	0.17
Al_2O_3											0.41	−0.37	−0.71	−0.56	0.33	0.45
Fe_2O_3												0.20	−0.75	−0.93	0.17	0.18
CaO													−0.26	−0.27	−0.22	−0.30
Sa														0.91	−0.17	−0.20
Saf															−0.18	−0.19
Bacteria																0.92
Fungi																

Significant correlations ($p < 0.05$). SOC: soil organic carbon; MOC: mineral-associated organic carbon. MAP: mean annual precipitation; MAT: mean annual temperature. Sa: silica-alumina ratio; Saf: silica-sesquioxide ratio.

The correlation between the MOC and minerals gradually increased with decreasing temperature (Table 4). Only Ver (r = 0.42) was significantly correlated with MOC in the highest temperature LP. Ver was the next most significantly correlated with MOC in the MP (r = 0.66). Chl (r = 0.75), Sme (r = 0.83), and It (r = 0.41) were significantly correlated with the MOC in the TP with the lowest temperature, and I/Sme (r = −0.73) was significantly negatively correlated with MOC.

Table 4. Pearson's correlation coefficients (r) among the MOC and clay minerals in different grassland transects.

	Kao	Chl	Sme	It	Ver	I/Sme
MP	−0.17	0.47	−0.24	−0.01	0.66 *	0.14
TP	0.62	0.75 *	0.83 **	0.41	−0.05	−0.73 **
LP	0.32	−0.13	0.12	0.10	0.42 *	−0.22

* $p < 0.05$, ** $p < 0.01$, significant correlations. Sme: smectite; It: illite; Ver: vermiculite; I/Sme: mixed-layer illite/smectite; Kao: kaolinite; Chl: chlorite.

The findings of the partial correlation study confirmed the significance of the MAP and MAT (Table 5). After controlling the effect of MAP, the relationship between the MOC and MAT changes from an insignificant to a significant negative correlation.

Table 5. Partial correlations between the SOC fractions and MAT after controlling the related soil properties in grassland transects.

	Zero-Order	MAP	pH	Clay
SOC	−0.25	−0.40 *	−0.08	−0.33
MOC	−0.26	−0.41 *	−0.10	−0.34

Zero-order: without controlling any factors. * $p < 0.05$, significant correlations. SOC: soil organic carbon; MOC: mineral-associated organic carbon. MAP: mean annual precipitation.

As for the spatial variation in different grassland transects, MOC accounted for 75% (Figure 5). The direct effect of the MAT and MAP on MOC is greater than the indirect effect. The MAT indirectly affects soil carbon stability by affecting CaO, clay particles, bacteria, etc. pH and Sa had negative effects on MOC. MAP, clay particles, and bacteria had

positive effects on MOC. The most significant factor influencing SOC was the pH, which was followed by bacteria.

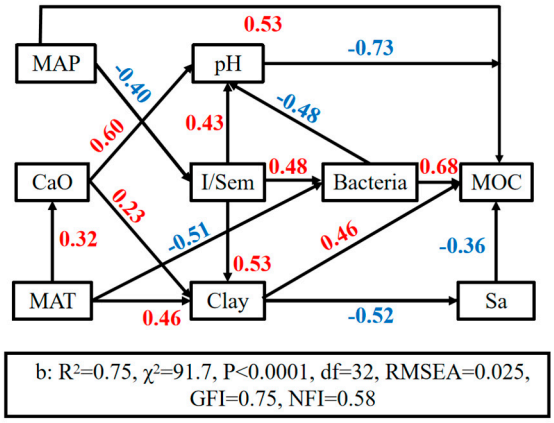

Figure 5. Structural equation model of the influence of environmental and soil factors on MOC. The numbers next to the path arrows indicate the standardized effect estimates and the direction of their relationship (Red for positive values, blue for negative values). MAP: mean annual precipitation; MAT: mean annual temperature; I/Sme: mixed-layer illite/smectite; MOC: minera-associated organic carbon; Sa: silica-alumina ratio.

4. Discussion

4.1. SOC and MOC in Grassland Soil Samples

Both the SOC and MOC contents of grassland soils decreased with increasing temperature (Figure 3a) [48]. This result was consistent with the findings that alpine grasslands are more likely to accumulate SOC [49]. Higher temperatures lead to higher soil temperatures, which activated microbial activity and accelerated the rate of SOC decomposition [50,51]. The SOC and MOC contents of grasslands other than the MP transect MS increased with increasing precipitation gradients in different grassland transects [52]. The study showed that precipitation has a positive effect on SOC accumulation. The impact of the kind of grassland on the variance in organic carbon storage was further examined in Wang's study [7]. The temperature precipitation gradient between the MP transect MS and the TS was less different compared to other transects. It has also been shown that the correlation between the loss of SOC and the increase in the MAT and MAP was stronger. However, the increase in SOC input was not sufficient to offset the loss due to more favorable decomposition conditions [53]. Therefore, the LP had the highest percentage of MOC and high SOC stability. However, its uptake was constrained by SOC. The MOC content was not the highest among the three sample strips. The lower the temperature is, the more sensitive the MOC content of the grassland transects was to changes in precipitation. The MOC content of MS soils in the MP was lower compared to other meadow grasslands. This was partly because changes in MOC may be related to the level of carbon input [9,33,54]. For example, precipitation can also increase SOC sequestration by promoting plant growth under certain conditions [8]. On the other hand, it may be related to a combination of conditions, such as the associated decomposition environment [54]. In arid and semi-arid grasslands, high soil water content can accelerate the rate of soil respiration, leading to SOC loss. The amount of water in the soil is a major factor in determining how the carbon cycle responds [16]. A recent study showed that under wet conditions, warming stimulates soil carbon uptake; under very dry conditions, warming inhibits carbon absorption [55]. The MOC/SOC content ranged from 65.33 to 66.67%, which is consistent with the results of Cai [23]. MOC/SOC increased with decreasing precipitation for the MP and LP and vice versa for the TP. The decomposition of soil organic carbon in high temperature and humid areas is usually not limited by soil water availability [53]. Therefore, water deficiency will limit carbon uptake and soil respiration, thus reducing MOC content [16].

4.2. Influence of Soil Physicochemical Properties on MOC

The pH in different grassland types increased with the decrease in the MAP except the MP transect MS. The pH increased with increasing temperature in all three grassland transects. The MOC content was negatively correlated with the pH ($r = -0.69$). To some extent, it explained the pattern of less MOC content in MP-MS. In terms of soil texture, we found significant differences in the clay content in the three transects. The MOC and SOC were positively correlated with the proportion of clay in the soil [56,57]. The MOC content can be enhanced by increasing carbon input. The moist soil with a higher fine silt content (soil, sand, and clay content) was more favorable for the accumulation of organic carbon. LP soils with high Sa and Saf values had the lowest weathering intensity. The content of clay grains and Fe/Al oxides gradually increased with increasing weathering intensity, which is in concordance with the findings in [58]. Also, metal oxides have been shown to be particularly effective in the sorption and stabilization of SOC [59,60]. The CaO content in LP soil was higher than the other two transects, which may be the reason for the highest MOC/SOC value in the LP transect. When CaO dissolves, calcium ions are released, which attach to soil particles and improve flocculation. Microaggregates may be formed in soils with a high clay content and cation exchange capacity [61], thus indirectly promoting organic carbon binding to minerals and improving SOC stability [62]. Also, the interaction between the pH and CaO had a positive effect on the stabilization of SOC [63]. It has been shown that the increase in calcium concentration in soils with a higher pH could effectively increase the attraction between clay and organic matter. Colloids could flocculate to a large extent due to electrostatic forces, which were the basis for the formation of agglomerates [64]. In agriculture, lime had been used to improve slabby soils [65,66], and CaO had also been added as an exogenous substance to soil amendments for application, thereby increasing the carbon sequestration capacity of soils [67].

4.3. Relationship between Clay Minerals and MOC

Among the three grassland transects, the highest content of Sme (2:1 swelling clay minerals) and It (2:1 non-swelling clay mineral) was the LP, and the lowest was the MP. The contents of Ver (2:1 swelling clay mineral) and I/Sme were the highest in MP soil. Studies have shown that soil (It, Sme, Ver) dominated by 2:1 type minerals has higher MOC content than soil (Kao) dominated by the 1:1 type [17]. Sme enhances SOC stability through its cationic bridge [68]. Ver as a 2:1 swelling mineral could improve SOC stability by stabilizing agglomerates [69]. The intercrystalline space of illite is full of low-hydrated K^+, and it is difficult to expand in water. Therefore, the ability to fix organic carbon is lower than Ver [70]. In contrast, I/Sme indirectly affected the MOC content by influencing the pH, clay content, and bacteria content (Figure 5). However, the correlation between MOC and mineral species differed at different temperature gradients, and the correlation between MOC and minerals gradually increased as the temperature decreased. Only Ver was positively correlated with MOC in the LP with the highest temperature. Therefore, the low Ver content was one of the reasons affecting the lowest MOC content in the LP. Ver was positively correlated with MOC in the MP. MOC in the TP with the lowest temperature was positively correlated with Sme and It. MOC was negatively correlated with I/Sme. To some extent, this explained the pattern of the highest MOC content in TP soils.

4.4. Comprehensive Effects of Climate, Soil Properties, and Minerals on MOC

SEM showed the formation of MOC because of physical and chemical interactions. One of the factors that had the greatest direct effect on MOC was the soil pH. An increase in the pH will lead to an increase in organic matter desorption and colloid mobilization, which may affect the stability of microaggregates [71]. The SOC in soil agglomerates was physically protected by the binding of minerals, leading to the inability of microorganisms to decompose them, thus increasing the MOC content [15]. SEM has shown that temperature has a significant impact on the dynamics of bacterial populations [72]. In addition, the composition of bacterial communities is closely related to MOC [73]. I/Sme can promote

the formation of MOC by influencing bacteria. Meanwhile, a few studies have noted that minerals were beneficial to the accumulation of soil microbial necrotic carbon, which was an important source of stable organic carbon [74]. The importance of climatic factors in controlling MOC has been recognized in a previous study [17]. Our results showed the strongest effect of the MAP on MOC [75]. Adequate soil moisture sustained plant growth so that plants further fixed SOC. On one hand, it ensures the input of carbon sources. On the other hand, it provides organic acids for root growth and microbial oxidative decomposition, reducing the pH value. It can be seen that there is a strong dependence between soil moisture, biomass production, and soil pH [76]. However, the effect of precipitation on MOC seems to obscure the role of other potential factors, such as the temperature, mineralogy, etc. [77]. I/Sme affected MOC by influencing clay mineral content in addition to the pH. The structure of clay minerals led to variable charges at their edges and these edges could form strong interactions with organic groups. Soils with a higher CaO content also had a higher pH, and CaO indirectly affected MOC by influencing the pH. In addition, soil oxides exhibited a high zero charge point. This enabled negatively charged organic groups to adsorb or react with permanently negatively charged clay minerals at most pH values below zero charges [78].

5. Conclusions

The variation of MOC and its relationship with clay minerals were studied in three typical grassland transects in China. It was found that the MOC contents of different transects were TP (14.89 g/kg) > MP (8.07 g/kg) > LP (5.41 g/kg). The MOC content was the result of a combination of the climate, soil properties, and minerals. Precipitation, as a climate factor, was positively correlated with MOC content ($r = 0.53$). Temperature correlated significantly ($r = 0.48$) with MOC after controlling for the effect of precipitation. Soil properties and minerals differed between grasslands affected by the climate. The pH of soil properties affected soil weathering and its ability to adsorb MOC. But in turn, the pH was also influenced by CaO and mixed-layer illite/smectite (I/Sme). The relationship between soil minerals and microorganisms in stabilizing organic carbon has also been found. Moreover, we also found a correlation between MOC and mineral species at different temperature gradients. As the temperature decreases, the correlation between MOC and minerals gradually increases. In summary, there was a coupling effect among organic carbon, soil properties, and clay mineral under natural climate change. The relationship between the above three factors cannot be simply explained by controlling one or two variables. The interaction between the influencing factors in the natural environment had to be comprehensively considered. In addition, the influence of clay minerals on MOC content varies with climate conditions, but not in all environments. Therefore, the influence of clay-grained minerals needed to be taken into account when studying SOC and its stability under certain conditions.

Author Contributions: Z.Z. and N.H. jointly designed the research; M.Z., M.L., and C.G. conducted the research; M.Z. wrote the manuscript; N.H. and J.Z. commented. All authors have read and agreed to the published version of the manuscript.

Funding: This work was supported by the Second Tibetan Plateau Scientifc Expedition and Research Program (2019QZKK0606-2), the International Cooperation Project of Science and Technology Department of Jilin Province, China (20220402061GH).

Institutional Review Board Statement: Not applicable.

Informed Consent Statement: Not applicable.

Data Availability Statement: The data presented in this study are available upon request from the corresponding author. The data are not publicly available due to laboratory regulations.

Conflicts of Interest: The authors declare no conflicts of interest.

References

1. Scurlock, J.M.O.; Hall, D.O. The global carbon sink: A grassland perspective. *Glob. Chang. Biol.* **1998**, *4*, 229–233. [CrossRef]
2. Schlesinger, W.H. *Biogeochemistry: An Analysis of Global Change*; Academic Press: San Diego, CA, USA, 1997. [CrossRef]
3. Abdalla, M.; Hastings, A.; Chadwick, D.R.; Jones, D.L.; Evans, C.D.; Jones, M.B.; Rees, R.M.; Smith, P. Critical review of the impacts of grazing intensity on soil organic carbon storage and other soil quality indicators in extensively managed grasslands. *Agric. Ecosyst. Environ.* **2018**, *253*, 62–81. [CrossRef]
4. Jiang, Z.Y.; Hu, Z.M.; Lai, D.Y.F.; Han, D.R.; Wang, M.; Liu, M.; Zhang, M.; Guo, M.Y. Light grazing facilitates carbon accumulation in subsoil in Chinese grasslands: A meta-analysis. *Glob. Chang. Biol.* **2020**, *26*, 7186–7197. [CrossRef] [PubMed]
5. Chen, Y.; Fischer, G. *A New Digital Georeferenced Data Base of Grassland in China*; IIASA Interim Report (IR-98-062); International Institute for Applied Systems Analysis (IIASA): Laxenburg, Austria, 1998. Available online: https://core.ac.uk/download/pdf/33897057.pdf (accessed on 15 February 2024).
6. Ni, J. Carbon storage in grasslands of China. *J. Arid. Environ.* **2002**, *50*, 205–218. [CrossRef]
7. Wang, S.P.; Wilkes, A.; Zhang, Z.; Chang, X.F.; Lang, R.; Wang, Y.; Niu, H.S. Management and land use change effects on soil carbon in northern China's grasslands: A synthesis. *Agric. Ecosyst. Environ.* **2011**, *142*, 329–340. [CrossRef]
8. Godde, C.M.; Thorburn, P.J.; Biggs, J.S.; Meier, E.A. Understanding the impacts of soil, climate, and farming practices on soil organic carbon sequestration: A simulation study in Australia. *Front. Plant Sci.* **2016**, *7*, 661. [CrossRef] [PubMed]
9. Luo, Z.K.; Baldock, J.; Wang, E.L. Modelling the dynamic physical protection of soil organic carbon: Insights into carbon predictions and explanation of the priming effect. *Glob. Chang. Biol.* **2017**, *23*, 5273–5283. [CrossRef]
10. Poeplau, C.; Don, A.; Six, J.; Kaiser, M.; Benbi, D.; Chenu, C.; Cotrufo, M.F.; Derrien, D.; Gioacchini, P.; Grand, S.; et al. Isolating organic carbon fractions with varying turnover rates in temperate agricultural soils-A comprehensive method comparison. *Soil Biol. Biochem.* **2018**, *125*, 10–26. [CrossRef]
11. Lawrence, C.R.; Schulz, M.S.; Masiello, C.A.; Chadwick, O.A.; Harden, J.W. The trajectory of soil development and its relationship to soil carbon dynamics. *Geoderma* **2021**, *403*, 115378. [CrossRef]
12. Cotrufo, M.F.; Ranalli, M.G.; Haddix, M.L.; Six, J.; Lugato, E. Soil carbon storage informed by particulate and mineral-associated organic matter. *Nat. Geosci.* **2019**, *12*, 989–994. [CrossRef]
13. Wang, X.; Wackett, A.A.; Toner, B.M.; Yoo, K. Consistent mineral-associated organic carbon chemistry with variable erosion rates in a mountainous landscape. *Geoderma* **2022**, *405*, 115448. [CrossRef]
14. Six, J.; Elliott, E.T.; Paustian, K.; Doran, J.W. Aggregation and soil organic matter accumulation in cultivated and native grassland soils. *Soil Sci. Soc. Am. J.* **1998**, *62*, 1367–1377. [CrossRef]
15. Lavallee, J.M.; Soong, J.L.; Cotrufo, M.F. Conceptualizing soil organic matter into particulate and mineral-associated forms to address global change in the 21st century. *Glob. Chang. Biol.* **2020**, *26*, 261–273. [CrossRef] [PubMed]
16. Zhao, F.B.; Wu, Y.P.; Hui, J.Y.; Sivakumar, B.; Meng, X.Y.; Liu, S.G. Projected soil organic carbon loss in response to climate warming and soil water content in a loess watershed. *Carbon Balance Manag.* **2021**, *16*, 24–38. [CrossRef]
17. Cai, A.D.; Xu, H.; Duan, Y.H.; Zhang, X.B.; Ashraf, M.N.; Zhang, W.J.; Xu, M.G. Changes in mineral-associated carbon and nitrogen by long-term fertilization and sequestration potential with various cropping across China dry croplands. *Soil Till Res.* **2020**, *205*, 104725. [CrossRef]
18. Wang, Z.G.; Govers, G.; Van Oost, K.; Clymans, W.; Van Den Putte, A.; Merckx, R. Soil organic carbon mobilization by interrill erosion: Insights from size fractions. *J. Geophys. Res. Earth Surf.* **2013**, *118*, 348–360. [CrossRef]
19. Luo, Z.K.; Rossel, R.A.V.; Shi, Z. Distinct controls over the temporal dynamics of soil carbon fractions after land use change. *Glob. Chang. Biol.* **2020**, *26*, 4614–4625. [CrossRef] [PubMed]
20. Zhao, Z.Z.; Zhao, Z.Y.; Fu, B.; Wang, J.G.; Tang, W. Characteristics of soil organic carbon fractions under different land use patterns in a tropical area. *J. Soil Sediment* **2020**, *21*, 689–697. [CrossRef]
21. Duan, Y.; Chen, L.; Li, Y.M.; Wang, Q.Y.; Zhang, C.Z.; Ma, D.H.; Li, J.Y.; Zhang, J.B. N, P and straw return influence the accrual of organic carbon fractions and microbial traits in a Mollisol. *Geoderma* **2021**, *403*, 115373. [CrossRef]
22. Li, Y.S.; Xie, Z.H.; Yu, Z.H.; Wang, Y.H.; Liu, C.K.; Wang, G.H.; Wu, J.J.; Jin, J.; Liu, X.B. Impact of surface soil manuring on particulate carbon fractions in relevant to nutrient stoichiometry in a Mollisol profile. *Soil Till Res.* **2021**, *207*, 104859. [CrossRef]
23. Cai, A.D.; Feng, W.T.; Xu, M.G. Climate, soil texture, and soil types affect the contributions of fine-fraction-stabilized carbon to total soil organic carbon in different land uses across China. *J. Environ. Manag.* **2016**, *172*, 2–9. [CrossRef]
24. Schweizer, S.A.; Mueller, C.W.; Hoschen, C.; Ivanov, P.; Kogel-Knabner, I. The role of clay content and mineral surface area for soil organic carbon storage in an arable toposequence. *Biogeochemistry* **2021**, *156*, 401–420. [CrossRef]
25. Feng, W.T.; Plante, A.F.; Six, J. Improving estimates of maximal organic carbon stabilization by fine soil particles. *Biogeochemistry* **2013**, *112*, 81–93. [CrossRef]
26. Lehmann, P.; Leshchinsky, B.; Gupta, S.; Mirus, B.B.; Bickel, S.; Lu, N.; Or, D. Clays are not created equal: How clay mineral type affects soil parameterization. *Geophys. Res. Lett.* **2022**, *48*, e2021GL095311. [CrossRef]
27. Kane, E.S.; Hockaday, W.C.; Turetsky, M.R.; Masiello, C.A.; Valentine, D.W.; Finney, B.P.; Baldock, J.A. Topographic controls on black carbon accumulation in Alaskan black spruce forest soils: Implications for organic matter dynamics. *Biogeochemistry* **2010**, *100*, 39–56. [CrossRef]
28. Yang, J.J.; Wang, J.; Li, A.Y.; Li, G.H.; Zhang, F. Disturbance, carbon physicochemical structure, and soil microenvironment codetermine soil organic carbon stability in oilfields. *Environ. Int.* **2020**, *135*, 105390. [CrossRef]

29. McNally, S.R.; Beare, M.H.; Curtin, D.; Meenken, E.D.; Kelliher, F.M.; Pereira, R.C.; Shen, Q.H.; Baldock, J. Soil carbon sequestration potential of permanent pasture and continuous cropping soils in New Zealand. *Glob. Chang. Biol.* **2017**, *23*, 4544–4555. [CrossRef] [PubMed]
30. Barre, P.; Fernandez-Ugalde, O.; Virto, I.; Velde, B.; Chenu, C. Impact of phyllosilicate mineralogy on organic carbon stabilization in soils: Incomplete knowledge and exciting prospects. *Geoderma* **2014**, *235*, 382–395. [CrossRef]
31. Traore, S.; Thiombiano, L.; Bationo, B.A.; Kogel-Knabner, I.; Wiesmeier, M. Organic carbon fractional distribution and saturation in tropical soils of West African savannas with contrasting mineral composition. *Catena* **2020**, *190*, 104550. [CrossRef]
32. Fukumasu, J.; Poeplau, C.; Coucheney, E.; Jarvis, N.; Kloffel, T.; Koestel, J.; Katterer, T.; Svensson, D.N.; Wetterlind, J.; Larsbo, M. Oxalate-extractable aluminum alongside carbon inputs may be a major determinant for organic carbon content in agricultural topsoils in humid continental climate. *Geoderma* **2021**, *402*, 115345. [CrossRef]
33. Bruun, T.B.; Elberling, B.; Christensen, B.T. Lability of soil organic carbon in tropical soils with different clay minerals. *Soil Biol. Biochem.* **2010**, *42*, 888–895. [CrossRef]
34. King, A.E.; Congreves, K.A.; Deen, B.; Dunfield, K.E.; Voroney, R.P.; Wagner-Riddle, C. Quantifying the relationships between soil fraction mass, fraction carbon, and total soil carbon to assess mechanisms of physical protection. *Soil Biol. Biochem.* **2019**, *135*, 95–107. [CrossRef]
35. Hu, P.L.; Zhang, W.; Wang, K.L. Soil carbon accumulation with increasing temperature under both managed and natural vegetation restoration in calcareous soils. *Sci. Total Environ.* **2021**, *767*, 145298. [CrossRef]
36. Wu, X.L.; Wei, Y.J.; Cai, C.F.; Yuan, Z.J.; Li, D.Q.; Liao, Y.S.; Deng, Y.S. Quantifying the contribution of phyllosilicate mineralogy to aggregate stability in the East Asian monsoon region. *Geoderma* **2021**, *393*, 115036. [CrossRef]
37. Wang, D.D.; Shi, X.Z.; Wang, H.J.; Weindorf, D.C.; Yu, D.S.; Sun, W.X.; Ren, H.Y.; Zhao, Y.C. Scale Effect of climate and soil texture on soil organic carbon in the uplands of northeast China. *Pedosphere* **2010**, *20*, 525–535. [CrossRef]
38. Zhou, Y.P.; Zhang, D.Z.; Zhang, J.J.; Zhao, M.S.; He, N.P. Changes in Soil Particulate Organic Carbon and Their Response to Changing Environments on the Tibetan Plateau, Mongolian Plateau, and Loess Plateau, China. *J. Soil Sci. Plant Nutr.* **2022**, *311*, 420–430. [CrossRef]
39. Yang, L.; Ning, D.; Yang, Y.; He, N.; Li, X.; Cornell, C.R.; Bates, C.T.; Filimonenko, E.; Kuzyakov, Y.; Zhou, J.; et al. Precipitation balances deterministic and stochastic processes of bacterial community assembly in grassland soils. *Soil Biol. Biochem.* **2022**, *168*, 108635. [CrossRef]
40. Chan, O.C.; Yang, X.; Fu, Y.; Feng, Z.; Sha, L.; Peter, C.; Zou, X. 16S rRNA gene analyses of bacterial community structures in the soils of evergreen broad-leaved forests in south-west China. *FEMS Microbiol. Ecol.* **2010**, *2*, 247–259. [CrossRef] [PubMed]
41. Liu, S.W.; Zhang, J.; Li, Q.G.; Zhang, L.F.; Wang, W.; Yang, P.T. Geochemistry and U-Pb zircon ages of metamorphic volcanic rocks of the Paleoproterozoic Lüliang Complex and constraints on the evolution of the TransNorth China Orogen, North China Craton. *Precambr. Res.* **2012**, *223*, 173–190. [CrossRef]
42. Manganese Brass Composition Analysis Standard Material GBW02103. Available online: http://www.gbw.org.cn/gbw114/yjgbw/GBW02103.html (accessed on 15 February 2024).
43. Wang, R.J.; Song, J.S.; Feng, Y.T.; Zhou, J.X.; Xie, J.Y.; Khan, A.; Che, Z.X.; Zhang, S.L.; Yang, X.Y. Changes in soil organic carbon pools following long-term fertilization under a rain-fed cropping system in the Loess Plateau, China. *J. Integr. Agric.* **2021**, *20*, 2512–2525. [CrossRef]
44. Cambardella, C.A.; Elliott, E.T. Particulate soil organic-matter changes across a grassland cultivation sequence. *Soil Sci. Soc. Am. J.* **1992**, *56*, 777–783. [CrossRef]
45. Zhang, Z.D.; Sheng, Q.N.; Zhao, M.S.; Zhong, J.J.; He, N.P.; Li, R.; Zhang, L.N.; Guo, D.; Zhang, J.J. Analysis of soil clay mineral in terrestrial ecosystem using X-ray diffraction spectroscopy. *Spectrosc. Lett.* **2021**, *54*, 65–71. [CrossRef]
46. Biscaye, P.E. Mineralogy and sedimentation of recent deep-sea clay in the Atlantic ocean and adjacent seas and oceans. *Bull. Geol. Soc. Am.* **1965**, *76*, 803–832. [CrossRef]
47. Lu, S.G.; Wang, S.Y.; Chen, Y.Y. Palaeopedogenesis of red palaeosols in Yunnan Plateau, southwestern China: Pedogenical, geochemical and mineralogical evidences and palaeoenvironmental implication. *Palaeogeogr. Palaeocl.* **2015**, *420*, 35–48. [CrossRef]
48. Lin, Z.B.; Zhang, R.D. Dynamics of soil organic carbon under uncertain climate change and elevated atmospheric CO_2. *Pedosphere* **2012**, *22*, 489–496. [CrossRef]
49. Yang, W.S.; Liu, Y.; Zhao, J.X.; Chang, X.F.; Wiesmeier, M.; Sun, J.; Lopez-Vicente, M.; Garcia-Ruiz, R.; Gomez, J.A.; Zhou, H.K.; et al. SOC changes were more sensitive in alpine grasslands than in temperate grasslands during grassland transformation in China: A meta-analysis. *J. Clean. Prod.* **2021**, *308*, 127430. [CrossRef]
50. Lu, M.; Zhou, X.H.; Li, B. Responses of ecosystem carbon cycle to experimental warming: A meta-analysis. *Ecology* **2013**, *94*, 726–738. [CrossRef] [PubMed]
51. Crowther, T.W.; Todd-Brown, K.E.O.; Rowe, C.W.; Wieder, W.R.; Carey, J.C.; Machmuller, M.B.; Snoek, B.L.; Fang, S.; Zhou, G.; Allison, S.D.; et al. Quantifying global soil carbon losses in response to warming. *Nature* **2016**, *540*, 104–110. [CrossRef]
52. Gottschalk, P.; Smith, J.U.; Wattenbach, M.; Bellarby, J.; Stehfest, E.; Arnell, N.; Osborn, T.J.; Jones, C.; Smith, P. How will organic carbon stocks in mineral soils evolve under future climate? Global projections using RothC for a range of climate change scenarios. *Biogeosciences* **2012**, *9*, 3151–3171. [CrossRef]
53. Heikkinen, J.; Keskinen, R.; Kostensalo, J.; Nuutinen, V. Climate change induces carbon loss of arable mineral soils in boreal conditions. *Glob. Chang. Biol.* **2022**, *28*, 3960–3973. [CrossRef]

54. Wang, S.Z.; Fan, J.W.; Zhong, H.P.; Li, Y.Z.; Zhu, H.Z.; Qiao, Y.X.; Zhang, H.Y. A multi-factor weighted regression approach for estimating the spatial distribution of soil organic carbon in grasslands. *Catena* **2019**, *174*, 248–258. [CrossRef]
55. Quan, Q.; Tian, D.S.; Luo, Y.Q.; Zhang, F.Y.; Crowthers, T.W.; Zhu, K.; Chen, H.Y.H.; Zhou, Q.P.; Niu, S.L. Water scaling of ecosystem carbon cycle feedback to climate warming. *Sci. Adv.* **2019**, *5*, 1131. [CrossRef] [PubMed]
56. Bosatta, E.; Ågren, G. Theoretical analyses of soil texture effects on organic matter dynamics. *Soil Biol. Biochem.* **1997**, *29*, 1633–1638. [CrossRef]
57. Rasmussen, C.; Heckman, K.; Wieder, W.R.; Keiluweit, M.; Lawrence, C.R.; Berhe, A.A.; Blankinship, J.C.; Crow, S.E.; Druhan, J.L.; Pries, C.E.H.; et al. Beyond clay: Towards an improved set of variables for predicting soil organic matter content. *Biogeochemistry* **2018**, *137*, 297–306. [CrossRef]
58. Dzemua, G.L.; Mees, F.; Stoops, G.; Van Ranst, E. Micromorphology, mineralogy and geochemistry of lateritic weathering over serpentinite in south-east Cameroon. *J. Afr. Earth Sci.* **2011**, *60*, 38–48. [CrossRef]
59. Barbera, V.; Raimondi, S.; Egli, M.; Plotze, M. The influence of weathering processes Mediterranean on labile and stable organic matter in volcanic soils. *Geoderma* **2008**, *143*, 191–205. [CrossRef]
60. Schrumpf, M.; Kaiser, K.; Mayer, A.; Hempel, G.; Trumbore, S. Age distribution, extractability, and stability of mineral-bound organic carbon in central European soils. *Biogeosciences* **2021**, *18*, 1241–1257. [CrossRef]
61. Keiblinger, K.M.; Bauer, L.M.; Deltedesco, E.; Holawe, F.; Unterfrauner, H.; Zehetner, F.; Peticzka, R. Quicklime application instantly increases soil aggregate stability. *Int. Agrophys.* **2016**, *30*, 123–128. [CrossRef]
62. Han, L.F.; Sun, K.; Jin, J.; Xing, B.S. Some concepts of soil organic carbon characteristics and mineral interaction from a review of literature. *Soil Biol. Biochem.* **2016**, *94*, 107–121. [CrossRef]
63. Seth, D.; Subudhi, S.; Rajput, V.D.; Kusumavathi, K.; Sahoo, T.R.; Dash, S.; Mangaraj, S.; Nayak, D.K.; Pattanayak, S.K.; Minkina, T.; et al. Exploring the role of mycorrhizal and rhizobium inoculation with organic and inorganic fertilizers on the nutrient uptake and growth of acacia mangium saplings in acidic soil. *Forests* **2022**, *12*, 1657. [CrossRef]
64. Getahun, G.T.; Etana, A.; Munkholm, L.J.; Kirchmann, H. Liming with $CaCO_3$ or CaO affects aggregate stability and dissolved reactive phosphorus in a heavy clay subsoil. *Soil Till Res.* **2021**, *214*, 105162. [CrossRef]
65. Li, Y.Y.; Feng, G.; Tewolde, H.; Zhang, F.B.; Yan, C.; Yang, M.Y. Soil aggregation and water holding capacity of soil amended with agro-industrial byproducts and poultry litter. *J. Soils Sediments* **2020**, *21*, 1127–1135. [CrossRef]
66. Gelsomino, A.; Petrovicova, B.; Zaffina, F.; Peruzzi, A. Chemical and microbial properties in a greenhouse loamy soil after steam disinfestation alone or combined with CaO addition. *Soil Biol. Biochem.* **2010**, *42*, 1091–1100. [CrossRef]
67. Nan, H.Y.; Yin, J.X.; Yang, F.; Luo, Y.; Zhao, L.; Cao, X.D. Pyrolysis temperature-dependent carbon retention and stability of biochar with participation of calcium: Implications to carbon sequestration. *Environ. Pollut.* **2021**, *287*, 117566. [CrossRef] [PubMed]
68. Wattel-Koekkoek, E.J.W.; Buurman, P.; Van Der Plicht, J.; Wattel, E.; Van Breemen, N. Mean residence time of soil organic matter associated with kaolinite and smectite. *Eur. J. Soil Sci.* **2003**, *54*, 269–278. [CrossRef]
69. Liu, M.; Han, G.L.; Zhang, Q. Effects of soil aggregate stability on soil organic carbon and nitrogen under land use change in an erodible region in southwest China. *Int. J. Environ. Res. Public Health* **2019**, *16*, 3809. [CrossRef] [PubMed]
70. Wang, C.; Li, F.C.; Shi, H.Z.; Jin, Z.D.; Sun, X.H.; Zhang, F.; Wu, F.; Kan, S. The significant role of inorganic matters in preservation and stability of soil organic carbon in the Baoji and Luochuan loess/paleosol profiles, Central China. *Catena* **2013**, *109*, 186–194. [CrossRef]
71. Ilg, K.; Dominik, P.; Kaupenjohann, M.; Siemens, J. Phosphorus-induced mobilization of colloids: Model systems and soils. *Eur. J. Soil Sci.* **2008**, *59*, 233–246. [CrossRef]
72. Rui, J.P.; Peng, J.J.; Lu, Y.H. Succession of bacterial populations during plant residue decomposition in rice field soil. *Appl. Environ. Microb.* **2009**, *75*, 4879–4886. [CrossRef]
73. Lian, T.X.; Jin, J.; Wang, G.H.; Tang, C.X.; Yu, Z.H.; Li, Y.S.; Liu, J.J.; Zhang, S.Q.; Liu, X.B. The fate of soybean residue-carbon links to changes of bacterial community composition in Mollisols differing in soil organic carbon. *Glob. Chang. Biol.* **2017**, *109*, 50–58. [CrossRef]
74. Ni, X.Y.; Liao, S.; Tan, S.Y.; Peng, Y.; Wang, D.Y.; Yue, K.; Wu, F.Z.; Yang, Y.S. The vertical distribution and control of microbial necromass carbon in forest soils. *Glob. Ecol. Biogeogr.* **2020**, *29*, 1829–1839. [CrossRef]
75. Guo, X.W.; Rossel, R.A.V.; Wang, G.C.; Xiao, L.J.; Wang, M.M.; Zhang, S.; Luo, Z.K. Particulate and mineral-associated organic carbon turnover revealed by modelling their long-term dynamics. *Soil Biol. Biochem.* **2022**, *173*, 108780. [CrossRef]
76. Kleber, M.; Eusterhues, K.; Keiluweit, M.; Mikutta, C.; Mikutta, R.; Nico, P.S. Mineral-organic associations: Formation, properties, and relevance in soil environments. *Adv. Agron.* **2015**, *130*, 1–140. [CrossRef]
77. Dixon, J.L.; Chadwick, O.A.; Vitousek, P.M. Climate-driven thresholds for chemical weathering in postglacial soils of New Zealand. *J. Geophys. Res.-Earth Surf.* **2016**, *121*, 1619–1634. [CrossRef]
78. Totsche, K.U.; Amelung, W.; Gerzabek, M.H.; Guggenberger, G.; Klumpp, E.; Knief, C.; Lehndorff, E.; Mikutta, R.; Peth, S.; Prechtel, A.; et al. Microaggregates in soils. *J. Plant Nutr. Siol Sci.* **2018**, *181*, 104–136. [CrossRef]